CrossMark

Comparative Study on Solid-State and Metastable Liquid-State Aging for SAC305/Cu Joints

Shuang Li[1] · Xiao-Wu Hu[1] · Wei-Guo Zhang[2] · Yu-Long Li[1] · Xiong-Xin Jiang[1]

Abstract

In order to study the influence of the physical state of solder on the interfacial reaction of dip-soldered Sn–3.0Ag–0.5Cu/Cu system, two kinds of experiments were designed, including: (1) solid-state aging between the solder and Cu substrate; (2) liquid-state aging between the metastable supercooled liquid-state solder and Cu substrate. The aging times were 30, 60, 120 and 180 min, respectively, and the aging temperature was 8 °C lower than the melting point of the Sn–3.0Ag–0.5Cu (SAC305) alloy (217 °C). The experimental data revealed that the physical state of the solder obviously affected the formation of the intermetallic compound (IMC), and resulted in the difference in the diffusion of atoms on the interface between the SAC305 solder and Cu substrate. The IMC interface after aging for 30 min presents unique characteristics compared with that of the sample after dip soldering. The IMC interface of solid-state aged SAC305/Cu couple is relatively planar, while the IMC interface under metastable supercooled liquid-state aging conditions presents scallop-like shape.

Keywords Lead-free solder · Supercooling · Metastable liquid state · Aging · Intermetallic compound

1 Introduction

With the continuous development of miniaturization of multi-functional electronic products, chips are getting smaller and more powerful. Serving conditions of electronic elements become more and more complicated. Therefore, under the current developing trend of electronic products, it is necessary and important to study the effects of thermal cycling and thermal aging on the formation, growth and mechanical properties of the micro-connected interface [1, 2]. Due to the destructive influence of Pb-containing solder on the environment, the application of lead-free solder alloy received a wide attention [3]. Sn–3.0Cu–0.5Ag (SAC305) solder possesses good performance in thermal fatigue and solderability, and it has been

widely used in microelectronics packaging [4–8]. SAC305 solder alloy has been widely considered as a representative lead-free solder. Cu is the most common metal substrate due to its low cost, availability and good solderability.

Currently, the researches on SAC305 solder mainly concentrate on microstructure, the growth kinetics of intermetallic compounds (IMCs) and the improvement of mechanical properties of joints [9–12]. Shen et al. [13] investigated the microstructure evolution and growth mechanism of the interfacial IMCs during the solid-state aging process. It was found that the grooves provided convenient channel for Cu atoms passing through the previous IMCs. The Cu atoms reacted with solder alloy to form IMC grains, and the total IMC thickness increased with increasing aging time. Li et al. [14] reported the microstructural evolution of the interfacial IMCs during solid-state aging process. They found that at the initial stage of solid-state aging, the Cu atoms in IMCs were primarily from the supersaturated solder alloys. When the Cu atoms came from supersaturated solder alloy were consumed, the Cu atoms for the further growth of IMCs were primarily from the Cu substrate. Subsequently, the gaps between scallops Cu_6Sn_5 IMCs were gradually blocked with the IMCs growing, resulting in a slower consumption rate of Cu substrate. Zhu et al. [15] studied

✉ Xiao-Wu Hu
huxiaowu@ncu.edu.cn

1   Key Lab for Robot and Welding Automation of Jiangxi Province, Mechanical and Electrical Engineering School, Nanchang University, Nanchang 330031, China

2   College of Mechanical and Electronic Engineering, Northwest A&F University, Yangling 712100, China

the effect of liquid-state aging on interfacial morphology of Sn-Cu solder joint. The results showed that the growth of IMC was controlled by diffusion mechanism during liquid-state aging process. And the diffusion coefficient was two orders of magnitude higher than that of solid-state aging. However, it is acknowledged that there is no comparison regarding the growth kinetics of the Cu_6Sn_5 phase between Cu substrate and metastable supercooled liquid solder or solid solder with the same temperature and composition. Thus, the main purpose of this study is to compare the differences in interfacial reaction between solid-state and metastable liquid-state SAC305 solders with Cu substrate at the same temperature.

For this purpose, we have performed specific differential scanning calorimeter (DSC) experiments of interfacial reactivity between metastable liquid SAC305 solder and Cu substrate as well as between solid SAC305 solder and Cu substrate rigorously at the same temperature of 209 °C. Afterward, a theoretical analysis of the interfacial reaction and the morphology of the reaction products are made in both experimental environments.

2 Experimental

In order to reveal the effect of the physical state of SAC305 solder on the growth kinetics and morphologies of interfacial intermetallic phases between solder and Cu substrate, we set up two experimental contents: (1) solid-state aging of the solid SAC305 solder/Cu substrate system; (2) liquid-state aging of metastable supercooled liquid-state SAC305 solder/Cu substrate system.

Cu substrate was obtained from electrolytic copper sheet (purity of 99.99%) with the dimension of 30 mm × 30 mm × 0.5 mm. It was successively cut, ground and finely polished with diamond paste and ultrasonically cleaned. Afterward, the Cu substrate was dipped into conventional liquid RMA flux for 1 s, followed by immersion in molten SAC305 solder filler metal at 250 °C for 3 s.

In order to control the physical state of the SAC305 solder and the accurate reaction temperature in the aging process, experiments (STA449F3) of differential scanning calorimetry (DSC) have been applied to execute these experiments. After the dip soldering process, we completely removed the solder on one side and then cut it into small pieces of approximately 3 mm × 3 mm. The sample is named "dip-soldered sheet" in the following experiments.

In the process of reflowing, the melting point, solidification temperature and undercooling of the solder need to be monitored. We put the dip-soldered sheet into alumina crucible and then put into the DSC equipment. The dipping conditions (temperature, time) were determined in order to obtain good wetting and received an intimate contact between the SAC305 solder and the pure Cu sheet.

Figure 1a shows the temperature profile of the simple reflow process for the dip-soldered sheet sample, including heating up to 280 °C and cooling down to room temperature at a cooling rate of 10 °C min⁻¹. Afterward, an exothermic peak was observed at about 201 °C during the cooling of the "dip-soldered sheet," as shown in Fig. 1a. This peak was due to the release of the solidification latent heat during the solidification of the solder after a classical reflow process. Figure 1a₁ presents the typical DSC curve observed during a reflow process of the "dip-soldered sheet," indicating that the solidification of the SAC305 solder occurs at about 201 °C and that the melting temperature of the solder is 217 °C. (The undercooling is about 18 °C.)

Figure 1b shows the temperature–time profile of SAC305/Cu-soldered samples under the conditions of liquid-state aging at 209 °C for 60 min, when the samples were heated up to 209 °C and annealed at this temperature for the aged time varying from 30 to 180 min. (The corresponding DSC curve is shown in Fig. 1b₁.) Figure 1c presents the time–temperature profile of SAC305/Cu-soldered samples under the conditions of metastable supercooled liquid-state aging at 209 °C for 60 min. For these experiments, in order to melt the SAC305, the "dip-soldered sheet" needs to be heated up to 250 °C and afterward to be cooled down to 209 °C. In order to reduce the temperature fluctuations, 5 °C min⁻¹ was set in heating process and 3 °C min⁻¹ in cooling process. All details concerning the DSC curves observed during these experiments are given in Fig. 1c₁. After each experiment, the exothermic peak was clearly detected in the case of a simple reflow process. If the exothermic peak was observed during cooling from 250 to 209 °C, the experiment should be considered as invalid. It meant that SAC305 solder solidified during the isothermal aging at 209 °C. After isothermally aged at 209 °C for the desired aging time, the sample temperature was cooled down to the room temperature. After that, the aged sample was cut into two pieces: one for observing the cross-sectional structure and another for the top view of the IMC morphologies under scanning electronic microscopy (SEM). The common metallographic practice was followed to reveal the cross-sectional view. To observe the top view of intermetallic compounds, majority of the solder was ground away.

The images were processed with image processing software by adjusting the contrast and brightness of the image, and then, the IMC layer was clearly separated and the pixel data of each layer of IMC were acquired. Through the following equation to obtain the interface layer IMC thickness (L_{IMC}):
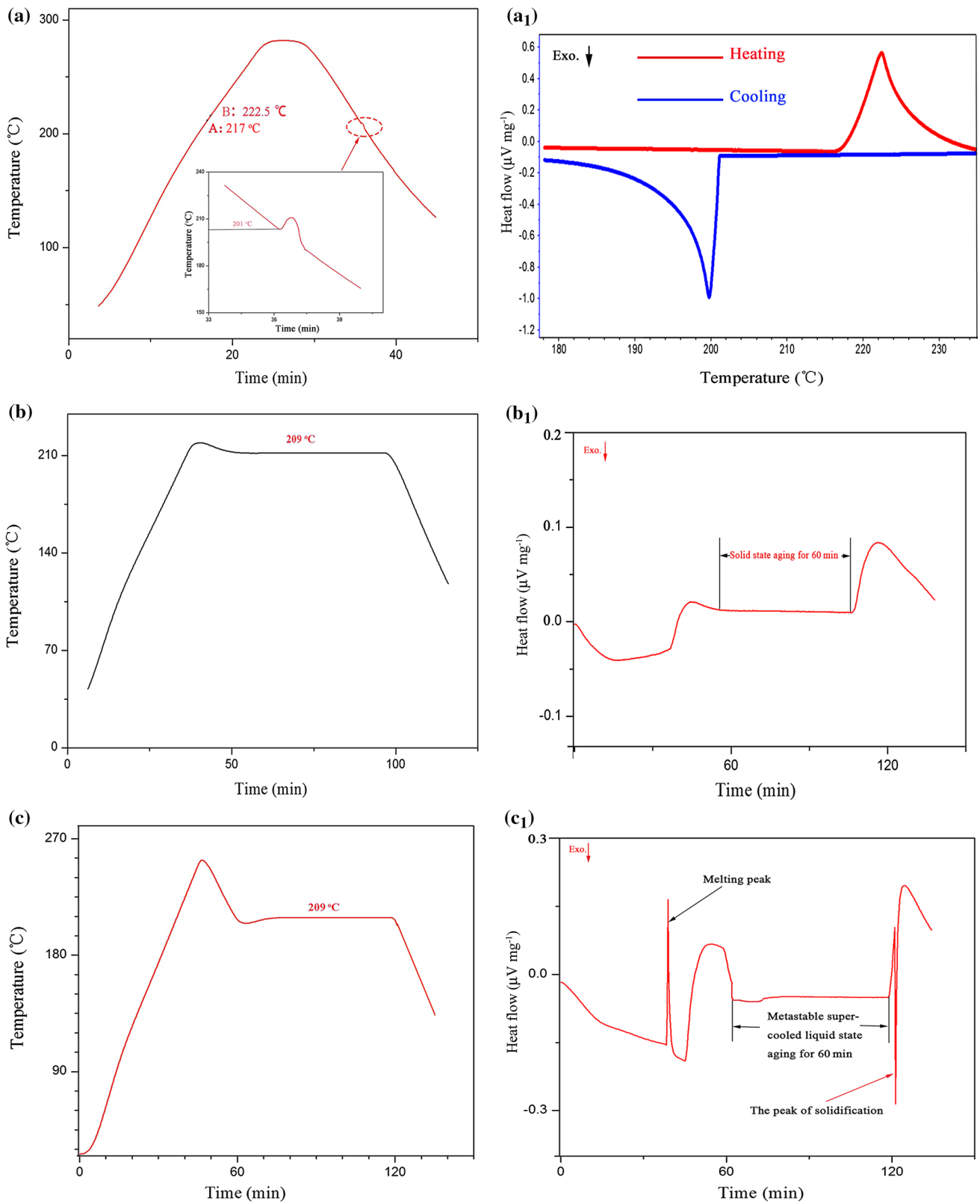
Fig. 1 Time–temperature curves **a**–**c** and exothermic curves **a₁**–**c₁** of SAC305/Cu-soldered samples under conditions of reflowing **a**, **a₁**, solid-state aging at 209 °C for 60 min **b**, **b₁** and metastable supercooled liquid-state aging at 209 °C for 60 min **c**, **c₁**

$$L_{IMC} = (N_{IMC}/N_{SEM}) \times L_{SEM}, \qquad (1)$$

where N_{IMC} is the pixel of the IMC layer, N_{SEM} is the total pixel of the SEM image, and L_{SEM} is the actual height of the SEM image.

The grain diameter of the Cu_6Sn_5 at the interface of SAC305/Cu solder joints was measured by the top view of micrographs. In order to ensure the accuracy of the measurement and to reduce the measurement error, the measurement of each set of data was at least 20 grains and then found the average.

3 Results and Discussion

3.1 Interfacial Microstructure Evolution

Figure 2a shows the interfacial SEM micrograph of the SAC305/Cu system after dip soldering at 250 °C for 3 s. The place with higher brightness in the picture is the SAC305 solder alloy, the middle layer is the interfacial IMCs, and the black part is the Cu substrate. In the study of SAC305 solder by Zimprich et al. [16], the scallop-like interfacial Cu_6Sn_5 IMC and a small amount of Cu_3Sn compound were formed at the interface of SAC305/Cu substrate soldered at 265 °C for 500 s. Those results indicate that the solid-state diffusion of interfacial elements is greatly dependent upon solder thickness during high temperature aging, that is, the thinner the solder layer is, the faster the Cu_3Sn layer grows. However, no Cu_3Sn was found at the interface of solder joints after dip soldering,

which could be owing to the short dip soldering time in this experiment. Figure 2b shows the cross-sectional microstructure of the solder joint aged under the solid state for 30 min. The endothermic peak of the DSC curve was not observed from the temperature–time profile in Fig. $1b_1$, thus ensuring that the sample was aged under solid-state conditions. Figure 2c shows the cross-sectional microstructure of the solder joint after aging for 30 min under the condition of metastable supercooled liquid state, and the energy-dispersive spectrometer (EDS) analysis results are shown in Fig. 2d, e. The experimental data showed that both Cu_6Sn_5 and Cu_3Sn formed at the SAC305/Cu interface. This phenomenon was similar to the previous research studied by Zimprich et al. [16]. An endothermic peak, corresponding to the reflow profile in Fig. $1c_1$ in the DSC curve, can be observed during the heating process, thus ensuring the solder is completely melted. Subsequently, an exothermic peak can be observed during its cooling down to room temperature. After thermal aging, the microstructural evolution of reaction interface became much different, compared with that only after dip soldering. The interface after solid-state aging for 30 min presented relatively plane, while the interface under the conditions of metastable supercooled liquid-state aging for 30 min presented scallop-like shape. Furthermore, another obvious phenomenon occurred in the metastable supercooled liquid-state aging for 30 min. Cu_3Sn intermetallic layer formed at Cu/SAC305 solder alloy interface, however, it did not form at the SAC305/Cu interface solid state aged for 30 min, but Cu_3Sn phase was observed after solid-state aging for 60 min. The Cu_6Sn_5 compounds have a high
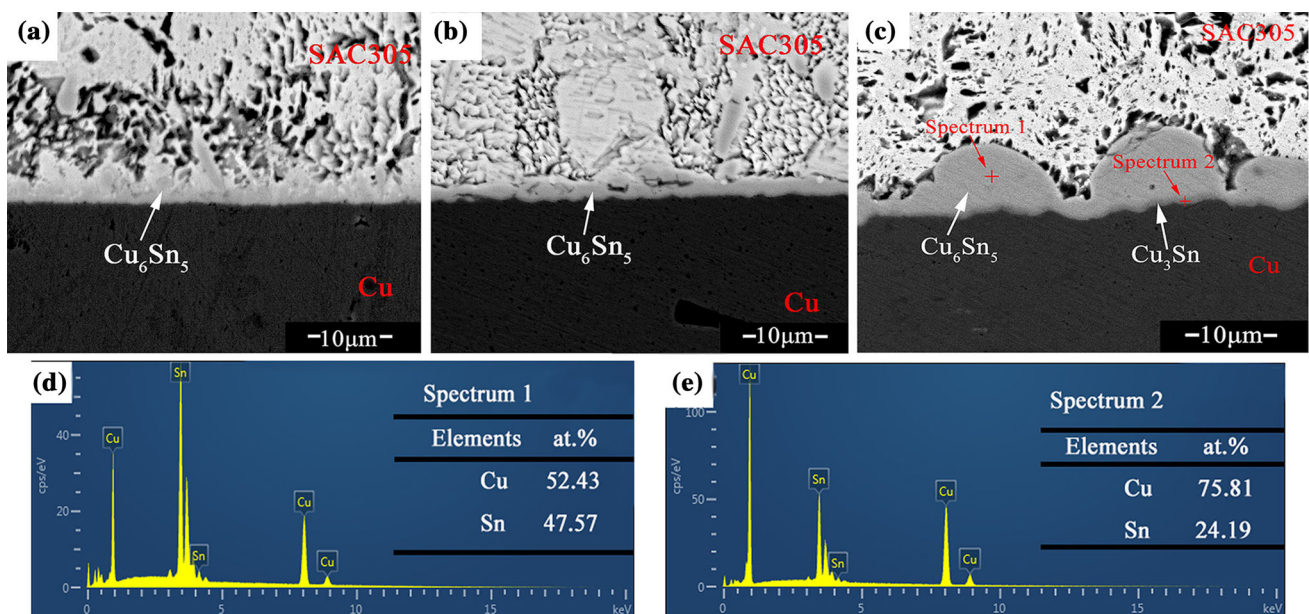

Fig. 2 Cross-sectional microstructures of SAC305/Cu solder joints after dip soldering for 3 s **a**, solid state aged for 30 min **b** and metastable supercooled liquid aged for 30 min **c** and EDS analysis of spectrums 1 **d** and 2 **e** from Fig. 1c
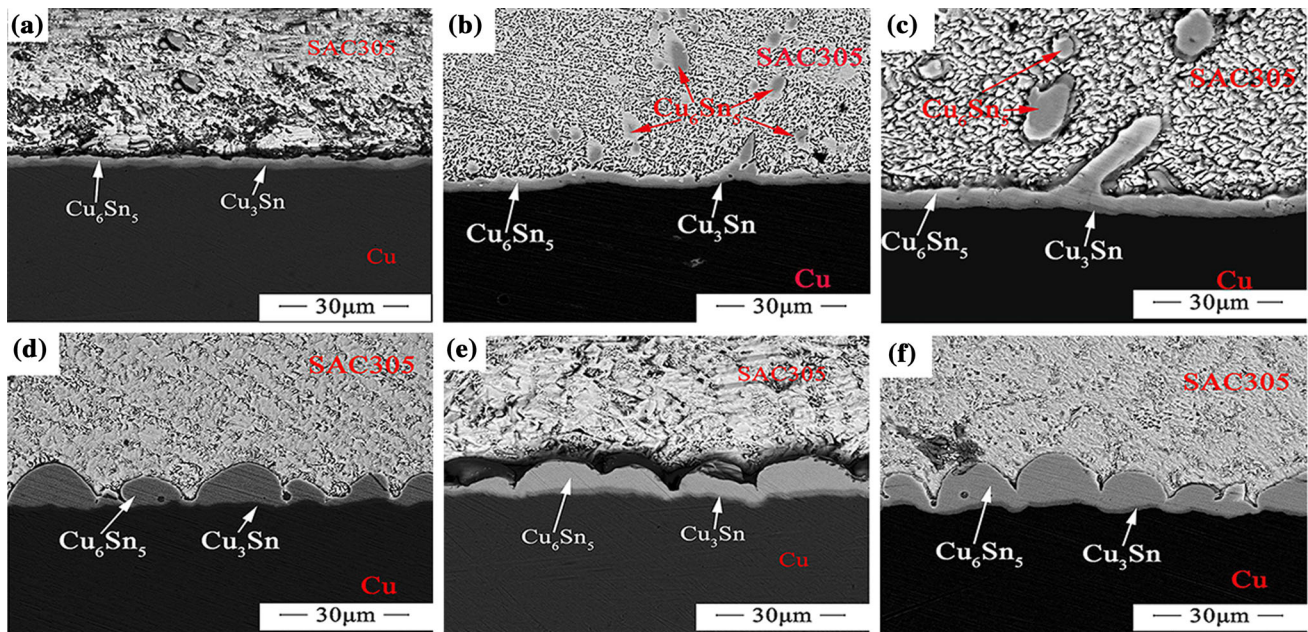
Fig. 3 Cross-sectional microstructures of SAC305/Cu solder joints under solid-state aging **a–c** and metastable supercooled liquid aging **d–f** for 60 min **a, d**, 120 min **b, e**, 180 min **c, f**

rate of formation under the metastable supercooled liquid state, and when this compound accumulates to a certain degree, it will react with Cu atoms on the substrate to form Cu_3Sn.

Figure 3a–c presents cross-sectional microstructures of SAC305/Cu solder joints aging under the solid state with aging time of 60, 120 and 180 min, respectively. Figure 3d–f presents cross-sectional views of the soldered sheets which were obtained by the reflow profile of Fig. 1c under the metastable supercooled liquid state, with aging time of 60, 120 and 180 min, respectively. It can be seen from the solid-state aged samples that a small amount of Cu_6Sn_5 phase is separated from the main interfacial IMC layer and embedded in the solder alloy. But this phenomenon cannot be observed during metastable supercooled liquid-state aging. The analysis results show that the interface wetting effect is better and the interface reaction rate between SAC305 solder and Cu substrate is faster during the liquid-state aging process. As a result, it is difficult for the Cu atoms on the substrate side to enter inside of the solder alloy through the initial IMC layer.

During the solid-state aging, the interface of the IMC layers presented relatively planar, while in the metastable supercooled liquid-state aging, the characteristic of the scalloped interface is obvious. During the liquid-state aging, the Cu atoms from substrate passed the nanochannels (Fig. 4) between the scalloped Cu_6Sn_5 phases and reacted with Sn atoms from solder, generating a new Cu_6Sn_5 phase and resulting in the rapid extension toward to the solder side [17]. The significant difference in
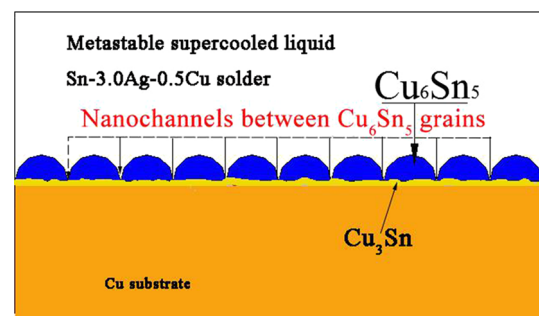

Fig. 4 Schematic diagram of nanochannels between Cu_6Sn_5 grains

the thickness of the interfacial IMC layers can be ascribed to two factors. One is that the Cu atoms could rapidly diffuse through liquid channels formed between some Cu_6Sn_5 scallops to react with Sn atoms. The existence of narrow channels between scallop-like Cu_6Sn_5 grains has been mentioned in previous literature [15]. Another one is that Cu atoms, diffusion in liquid solder is faster than that in the solid solder (according to Refs. [8, 18, 19]), resulting in that the thicknesses of the interface layers were significantly different for liquid-state aged joints.

Figure 5 depicts the X-ray diffraction (XRD) profile of the SAC305/Cu solder joint interface. It was observed that four types of phases, including β-Sn, Cu_6Sn_5, Ag_3Sn and Cu phases, were found. Figure 6 presents the morphologies of interfacial compounds grains in SAC305/Cu solder joints under different physical states. Compared to that of solid-state aging, grains size under the aging condition of the metastable supercooled liquid state was greater.
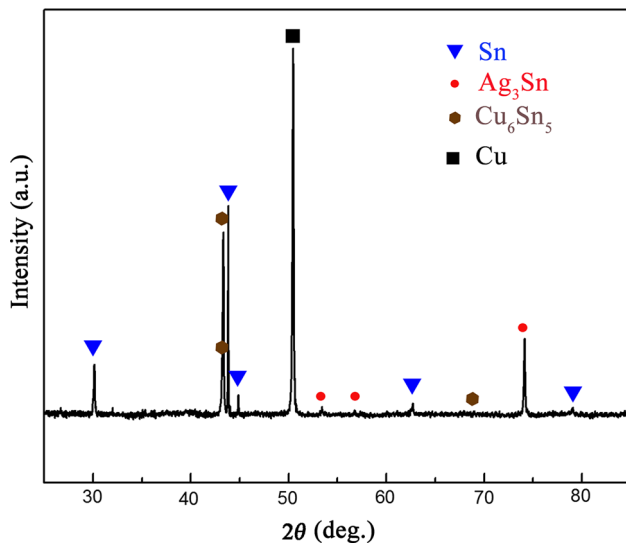
Fig. 5 XRD pattern of SAC305/Cu solder joint aged at 209 °C for 60 min under supercooled metastable liquid-state condition

Furthermore, it can be seen from Fig. 6 that the Ag_3Sn grains are embedded in the Cu_6Sn_5 grains boundary during the solid-state aging, while during the process of metastable liquid aging, Ag_3Sn grains are attached on the surface of Cu_6Sn_5 grains, thus indicating that there are significant differences in grain growth mechanism between the two physical states. There are two main reasons to explain this microscopic morphology difference. On the one hand, the liquidity of Ag_3Sn in liquid solder is better than that in solid solder. Under the aging condition of solid state, Ag_3Sn is enriched in the edge of Cu_6Sn_5 grain boundary, which makes the grain boundary obtain more resistance for atom diffusion and the grain coalescence is slowed down. However, the interface of SAC305/Cu joint under the condition of metastable supercooled liquid–state aging, the enrichment of Ag_3Sn at the grain boundaries of Cu_6Sn_5 is relatively low degree, which makes the grain boundary obtain lower resistance for atom diffusion, resulting in obvious differences in grain size between the solid-state aging and supercooled metastable liquid-state aging. On the other hand, it is difficult for the Cu atoms from the substrate passed through the initial IMC layers and reacted with Sn atoms from solder to formed new Cu_6Sn_5 compound during the solid-state aging. Due to the limited supply of Cu atoms for growth of Cu_6Sn_5 IMC, grain growth was impeded during the solid-state aging process. In contrast, due to the better interfacial solderability and the presence of nanochannels, the Cu atoms from the substrate passed through the IMC layers and reacted with the Sn atoms from the solder more intensely during the metastable supercooled liquid-state aging process, which resulted in the sufficient supply of Cu atoms for coarsening of Cu_6Sn_5 grains.
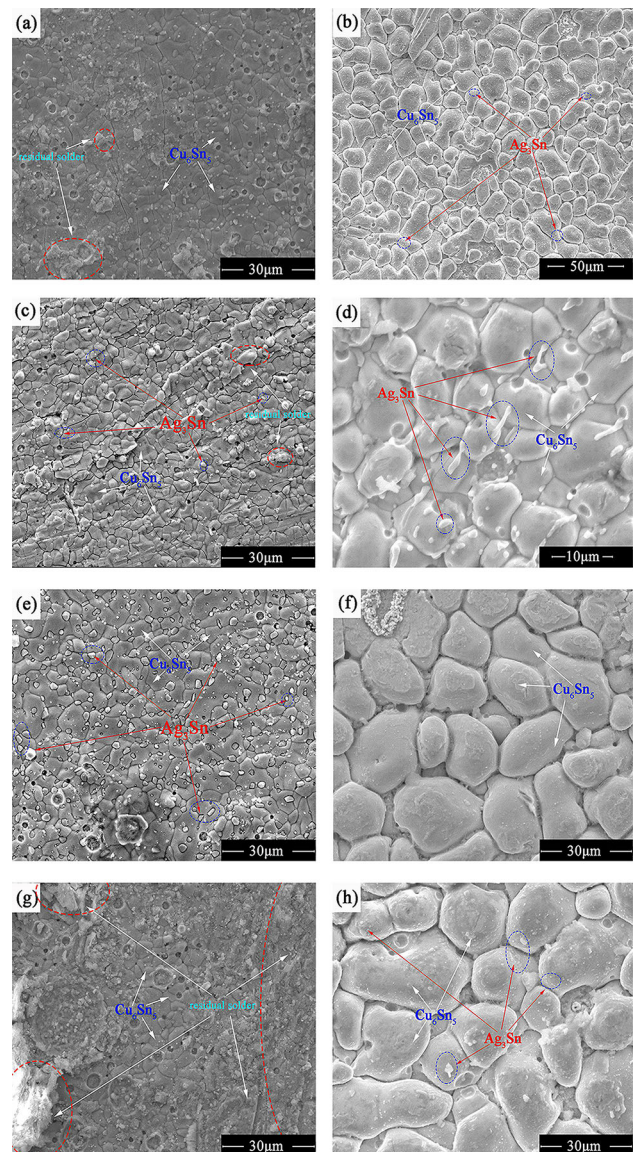

Fig. 6 Morphologies of SAC305/Cu interfacial compound grains aged at 209 °C under conditions of solid-state aging **a**, **c**, **e**, **g** and metastable supercooled liquid aging **b**, **d**, **f**, **h** for 30 min **a**, **b**, 60 min **c**, **d**, 120 min **e**, **f**, 180 min **g**, **h**

The interfacial IMC layer thickness was obtained from their cross section of micrographs, and the results are listed in Table 1. The thicknesses of IMCs layers were 3.17, 3.84, 4.41 and 4.87 µm for the SAC305/Cu solder joints aged for 30, 60, 120 and 180 min under the condition of solid state, respectively. However, when the samples were aged under the metastable supercooled liquid state for the same time, the thicknesses of IMCs layers were 6.25, 9.53, 11.27 and 12.23 µm, respectively. When the solder sheets were aged at different physical states, the thickness of IMCs layers increased with increasing aging time. But the physical state of the solder is one of the important factors affecting the

**Table 1** IMC thickness (μm) with increasing aging time under various aging state

Aging time (min)	Solid-state aging	Metastable supercooled liquid aging
30	3.17	6.25
60	3.84	9.53
120	4.41	11.27
180	4.87	12.23

thickness of the IMCs layers. Under metastable super-cooled liquid-state aging, IMC layer is 2.5–4.8 times thicker than that in the case of solid-state aging. Despite the solder at the same temperature with different of physical state, due to the better interfacial solderability and the presence of nanochannels (as shown in Fig. 4), the Cu atoms from the substrate passed through the IMCs layer and reacted with the Sn atoms from the solder more intensely in metastable supercooled liquid state. In contrast, since the solid-state diffusion rate of the Cu atoms was relatively slow, it would limit the growth of the IMC layers during the solid-state aging. As a result, these above-mentioned differences would result in that the thicknesses of the formed interfacial IMC layers were significantly different. Those results were similar to the conclusions proposed by Liashenko et al. [17].

The thickness of the IMC layer at the interface of the solder joint is related to the aging time. The relationship can be expressed by a power formula [13, 20]:

$$X = X_0 + At^n, \tag{2}$$

where X is the thickness of the IMC layers, X_0 is the initial thickness of the IMC layers, A is the growth rate constant, and n is the time index. Figure 7 shows the linear relationship between the total IMC thicknesses on SAC305/Cu interfaces and the square root of aging time. The error bars of the IMC equivalent thickness were obtained using the
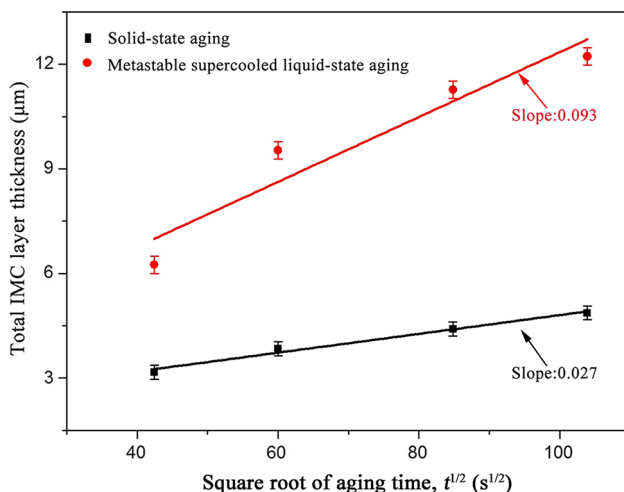
Fig. 7 Relationships of total IMC thickness on SAC305/Cu interfaces with square root of aging time on different aging conditions

stand deviation function from the measured data. In this case, $n = 0.5$, while the slope of the fitted straightening about solid state and the metastable supercooled liquid aging was 0.027 and 0.093, respectively. The growth rate constant of the solid-state aging treatment was 7.29×10^{-16} m^2 s^{-1}, while in the process of metastable supercooled liquid aging the growth rate constant was 8.65×10^{-15} m^2 s^{-1}. During this solid-state aging process, the interface IMC growth rate of SAC305/Cu solder joints was close to that reported by Li et al. [21]. Table 2 shows the average grain diameter after aging in different physical states. When the dip solder sheets were solid state aged for 30, 60, 120 and 180 min, the average grain diameters were 3.87, 4.84, 5.25 and 5.88 μm, respectively. However, when they were under the metastable supercooled liquid-state aging, these were 10.69, 13.60, 16.28 and 21.08 μm, respectively. The comparison of the two sets of data is made and shows that the diameter of the grains increased with increasing aging time. Compared to that of solid-state aging, the grains sizes of interfacial IMCs under the metastable supercooled liquid-state aging were 3–4 times higher.

The growth behavior of IMC grain size is usually expressed as follows [22, 23]:

$$d = Ct^k, \tag{3}$$

where d is the average diameter of the Cu_6Sn_5 grains, C is a constant, k is the time index, and t is the aging time.

Take the logarithm of both sides of Eq. (2):

$$\ln d = C_1 + k \ln t, \tag{4}$$

where C_1 is a constant. As can be seen from Fig. 8, when the soldered sheets are aged under the condition of metastable supercooled liquid state, the slope of the straight line is 0.3371. In the solid-state aging, the slope of the straight line is 0.22149, which deviates from the theory that the theoretical IMC grain size should be proportional to the cube root of time ($k = 1/3$). This may be attributed to the grain growth affected by interfacial reaction and atomic interdiffusion [24]. The growth rate of the grain is faster when aging under liquid condition, comparing to solid-state aging. In the previous study [22, 25, 26], researchers proposed a flux-driven ripening (FDR) theory to study the coarsening behavior of interfacial Cu_6Sn_5 grains under solid-state aging conditions. In addition, the value of

Table 2 Average grain diameter (μm) with increasing aging time under various aging state

Aging time (min)	Solid-state aging	Metastable supercooled liquid aging
30	3.87	10.69
60	4.84	13.60
120	5.25	16.28
180	5.88	21.08
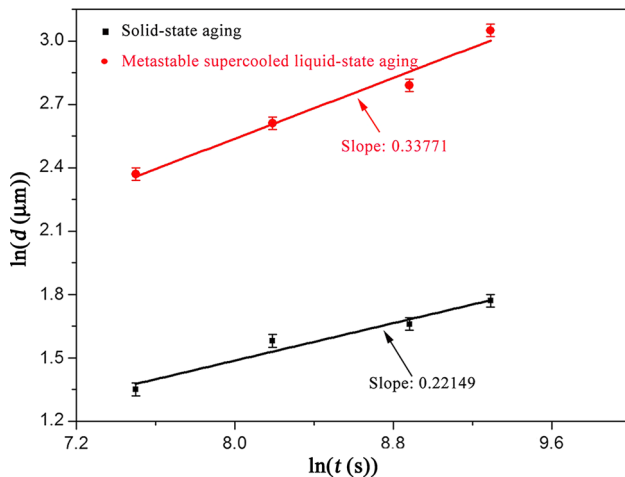
Fig. 8 Plots of Cu_6Sn_5 grain mean diameters (d) versus aging time (t) on logarithm coordinates at different physical state

k exponent was calculated to be 0.28, which is close to 1/3, whereas, under the assumption given by the FDR model, Cu_6Sn_5 grains were hemispherical, coarsened by merging near grains. It can be ascribed to the Gibbs–Thomson effect, which results in that the Cu concentration near the surface of smaller grains is higher and Cu atoms in smaller grains are apt to merge into the molten solder and spread into larger one. And during the liquid-state aging, the Cu influences the coarsening of interfacial Cu_6Sn_5 grains.

Contrastively, during the solid-state aging, the change of hemispherical grains occurs. Moreover, the various diffusion pathways for Cu atoms are presented in the case of solid-state aging. As a result, it should be considered that the coarsening mechanism for interfacial IMCs under solid-state aging is different from that under liquid-state aging, when aged under solid-state conditions, the k value is 0.22149, a significant departure from 1/3.

4 Conclusions

(1) It can be seen from the solid-state aged samples that a small amount of Cu_6Sn_5 phase is separated from the main interfacial IMC layer and embedded in the solder alloy. But this phenomenon cannot be observed during metastable supercooled liquid-state aging. The analysis results show that the interface wetting effect is better and the interface reaction rate between SAC305 solder and Cu substrate is faster during the liquid-state aging process. As a result, it is difficult for the Cu atoms on the substrate side to enter the inside of the solder alloy through the initial IMC layer.

(2) The liquidity of Ag_3Sn in liquid solder is better than that of solid solder. Under the aging condition of solid state, Ag_3Sn is aggregated at the edge of Cu_6Sn_5 grain boundary, which makes the grain boundary obtain more resistance for atom diffusion and the grain growth rate is slower. However, under the condition of metastable supercooled liquid state, the amount of Ag_3Sn at the grain boundaries of Cu_6Sn_5 relatively decreases, which weaken the resistance for atom diffusion, resulting in obvious differences in the grain size between the solid-state aging and supercooled metastable liquid-state aging.

(3) The coarsening mechanisms of interfacial Cu_6Sn_5 grains in solid-state and liquid-state reactions are different. In the FDR model, the aging under liquid-state Cu_6Sn_5 grains is assumed to be hemispherical. During the solid-state aging process, the pattern of hemispherical grains changes and the diffusion paths of Cu atoms are different from those of liquid solder.

References

[1] C.Y. Lin, C.C. Jao, C. Lee, Y.W. Yen, J. Alloys Compd. **440**, 333 (2007)
[2] L. Zhang, L.L. Gao, J. Alloys Compd. **635**, 55 (2015)
[3] C.W. Huang, K.L. Lin, Mater. Trans. JIM **45**, 588 (2004)
[4] X.W. Hu, T. Xu, K. Li, Y.L. Li, X.X. Jiang, J. Alloys Compd. **690**, 720 (2017)
[5] O.M. Abdelhadi, L.L. Ladani, J. Alloys Compd. **537**, 87 (2012)
[6] H.B. Qin, X.P. Zhang, X.B. Zhou, J.B. Zeng, Y.W. Mai, Mater. Sci. Eng. A **617**, 14 (2014)
[7] W.Q. Peng, E. Monlevade, M.E. Marques, Microelectron. Reliab. **47**, 2161 (2007)
[8] X.J. Wang, Y.L. Wang, F.J. Wang, N. Liu, J.X. Wang, Acta Metall. **27**, 1159 (2014)

[9] A.M. Gusak, K.N. Tu, Phys. Rev. B **66**, 115403 (2002)

[10] X.X. Tu, D.Q. Yi, J. Wu, B. Wang, J Alloys Compd. **698**, 317 (2017)

[11] Q.S. Zhu, Z.F. Zhang, J.K. Shang, Z.G. Wang, Mater. Sci. Eng. A **435–436**, 588 (2006)

[12] D.Z. Li, C.Q. Liu, P.P. Conway, J. Electron. Mater. **35**, 388 (2006)

[13] J. Shen, M.L. Zhao, P.P. He, Y.Y. Pu, J. Alloys Compd. **574**, 451 (2013)

[14] H.L. Li, R. An, C.Q. Wang, Z. Jiang, J. Alloys Compd. **634**, 94 (2015)

[15] X.O. Zhu, L. Zhao, S. Tian, Y. Zhou, Electron. Compon. Mater. **35**, 67 (2016)

[16] P. Zimprich, A. Betzwar-Kotas, G. Khatibi, B. Weiss, H. Ipser, J. Electron. Mater. **19**, 383 (2008)

[17] O.Y. Liashenko, F. Hodaj, Acta Mater. **99**, 106 (2015)

[18] S.W. Chen, Y.W. Yen, J. Electron. Mater. **28**, 1203 (1999)

[19] J.O. Suh, K.N. Tu, G.V. Lutsenko, A.M. Gusak, Acta Mater. **56**, 1075 (2008)

[20] P.T. Vianco, J.A. Rejent, J. Electron. Mater. **33**, 991 (2004)

[21] X.Y. Li, F.H. Li, F. Guo, Y.W. Yao, J. Electron. Mater. **40**, 51 (2011)

[22] H.K. Kim, K.N. Tu, Phys. Rev. B **53**, 593 (1996)

[23] Ming Yang, Mingyu Li, Jongmyung Kim, Intermetallics **31**, 177 (2012)

[24] Y. Tang, G.Y. Li, Y.C. Pan, J. Alloys Compd. **554**, 195 (2013)

[25] H.F. Zou, H.J. Yang, Z.F. Zhang, Mater. Chem. Phys. **131**, 190 (2011)

[26] A.M. Gusak, K.N. Tu, Phys. Rev. B **66**, 115403 (2002)